Coastline segmentation on Landsat 8 OLI images using majority voting with deep learning models

Nur Nafiiyah[1], Salwa Nabilah[2], Nur Azizah Affandy[2], Rifky Aisyatul Faroh[3], Esa Prakasa[4]
[1]Department of Informatics, Universitas Islam Lamongan, Lamongan, Indonesia
[2]Department of Civil Engineering, Universitas Islam Lamongan, Lamongan, Indonesia
[3]Department of Electrical Engineering, Universitas Islam Lamongan, Lamongan, Indonesia
[4]Research Center for Data Science and Information, National Research and Innovation Agency (BRIN), Jakarta, Indonesia

Article Info

Article history:

Received Sep 23, 2025
Revised Mar 31, 2026
Accepted Apr 15, 2026

Keywords:

Deep learning
Landsat 8 OLI
Majority voting
Segmentation automation
Segmentation coastline

ABSTRACT

Coastlines are highly dynamic due to both natural processes and anthropogenic factors, including global warming and sea level rise. Accurate coastline segmentation is essential for effective monitoring and management. Although previous studies have applied deep learning for coastline detection, many existing models still suffer from instability across scenes, blurred boundaries, and segmentation artifacts, indicating that model generalization remains a challenge. This study aims to develop a more robust coastline segmentation approach by introducing an automated majority voting strategy that integrates three deep learning models: ResNet50, ResNet18, and MobileNet-V2. Landsat 8 OLI imagery is used for training and testing. The Jaccard index results show that ResNet18, ResNet50, and MobileNet-V2 achieved scores of 0.96, 0.98, and 0.95 respectively, while the proposed majority voting method also achieved 0.98. Despite the producing a similar numerical score to the best individual model (ResNet50), the ensemble method improves segmentation consistency by reducing artifacts such as unwanted peripheral shapes and cracks within land areas. These findings demonstrate that combining multiple segmentation outputs yields more stable and reliable coastline detection than using single models. Future work will apply this approach to broader Indonesian coastal regions to further assess its generalizability across diverse shoreline conditions.

Corresponding Author:

Nur Nafiiyah
Department of Informatics, Universitas Islam Lamongan
Veteran 53A Street, Lamongan, Indonesia
Email: mynaff@unisla.ac.id

1. INTRODUCTION

Coastal areas are continuously changing due to abrasion, accretion, sea level rise, and anthropogenic pressures such as global warming and coastal development [1], [2]. Monitoring these changes is crucial for conservation, planning, and sustainable management. Remote sensing provides an efficient approach to detect coastline dynamics without direct field surveys.

Landsat 8 OLI imagery has become widely used for coastline studies, supporting research on automatic land-sea segmentation [3], [4], machine learning approaches [3], [5], coastline extraction [6]–[9], and practical applications such as navigation and landing [10]–[12]. However, these methods continue to face difficulties in distinguishing land from water in scenes with strong spectral similarity, image noise, and low contrast. These limitations often reduce the precision and stability of resulting coastline boundaries.

Deep learning methods, particularly convolutional neural networks (CNNs), have demonstrated strong performance in image classification and segmentation tasks [1]. Several architectures, including encoder-decoder models [13]–[15], U-Net [16]–[18], bi-LSTM [19], ensemble learning [20], and MobileNet-V2 [21], have been applied to coastline segmentation. Although these models improve feature extraction on low-resolution imagery [22]–[24], individual models still struggle to produce robust and artifact-free results across diverse coastal conditions.

Ensemble approaches have been explored in previous studies and have show potential for improving segmentation consistency [5], [7]. In various domains such as medical imaging, remote sensing classification, and road extraction, ensemble deep learning through techniques like majority voting or feature level fusion has been demonstrated to enhance boundary precision and reduce noise related artifacts, particularly in cases with ambiguous or low contrast features. However, existing ensemble studies have not specifically evaluated the integration of ResNet50, ResNet18, and MobileNet-V2 for coastline segmentation, despite their effectiveness in other fields [25]. Moreover, no prior research has systematically tested majority voting ensembles for coastline segmentation using Landsat 8 OLI, leaving a gap in understanding whether combining multiple models can mitigate boundary noise and improve robustness across diverse shoreline conditions.

To address this gap, this study proposes an automated coastline segmentation method based on a majority voting strategy that integrates ResNet50, ResNet18, and MobileNet-V2. The aim is to enhance segmentation reliability by reducing artifacts and producing more consistent coastline boundaries than those generated by individual deep learning models. This approach is expected to offer a more stable alternative for operational coastline monitoring.

2. RESEARCH METHOD

2.1. Dataset

This study uses a publicly available dataset from research [7], accessible at http://www.remotesensinglab.yildiz.edu.tr. From this dataset, 824 images were selected for training and 20 images for testing. Each image has a resolution of 224 × 224 pixels, with white pixels representing seawater and black pixels representing land. The dataset is derived from Landsat 8 OLI imagery, which provides multispectral, atmospherically corrected, and temporally consistent data suitable for coastline extraction. The use of Landsat imagery is particularly significant because its global coverage and long-term continuity support reproducible and scalable coastline monitoring. Before model training, several preprocessing steps were applied, including resizing all images to a uniform resolution and ensuring consistent alignment between input images and ground-truth masks. No additional enhancement techniques, such as histogram equalization or noise filtering, were used to preserve the original spectral characteristics of coastal boundaries.

2.2. Proposed method

The selection of ResNet50, ResNet18, and MobileNet-V2 was based on their balance of accuracy, computational efficiency, and proven effectiveness in transfer learning applications. ResNet architectures were chosen because their residual connections help mitigate the vanishing gradient problem and enable deeper feature extraction. MobileNet-V2 was included as a lightweight alternative designed for efficient computation. Although other transfer learning CNNs such as VGG and DenseNet are available, this study focuses on evaluating representative heavy, medium, and lightweight architectures to analyze their behavior within an ensemble. Future studies may incorporate additional TL-CNNs to expand the comparative analysis.

ResNet50 is a 50-layer convolutional neural network pretrained on ImageNet and capable of classifying images into 1000 object categories, allowing it to learn rich and transferable feature representations [13]. ResNet18 is a smaller 18-layer version that retains the residual learning mechanism but with fewer parameters, also benefiting from ImageNet pretraining to support robust feature extraction [13]. MobileNet-V2 is a 53-layer lightweight CNN based on inverted residual blocks and depthwise separable convolutions, and its pretrained ImageNet weights enable effective generalization to new image segmentation tasks [13]. All pretrained models thus leverage ImageNet-based initialization to improve convergence and performance. This research proposes a coastline segmentation method that distinguishes seawater and land using deep learning convolutional neural networks, following the approach introduced in study [7]. In that study, the WaterNet model combined outputs from several deep learning segmentation architectures. Similarly, the present work applies an ensemble strategy by combining the segmentation results of ResNet50, ResNet18, and MobileNet-V2 using a majority voting mechanism, where the final class for each pixel is determined by the most frequent prediction among the three models. Figure 1 illustrates the proposed segmentation workflow.

Model performance is evaluated using the Jaccard Similarity Coefficient, as shown in (1). In this equation, A represents the predicted segmentation mask produced by the model, and B represents the ground-truth label. This metric quantifies the overlap between prediction and reference and is widely used in semantic segmentation tasks.

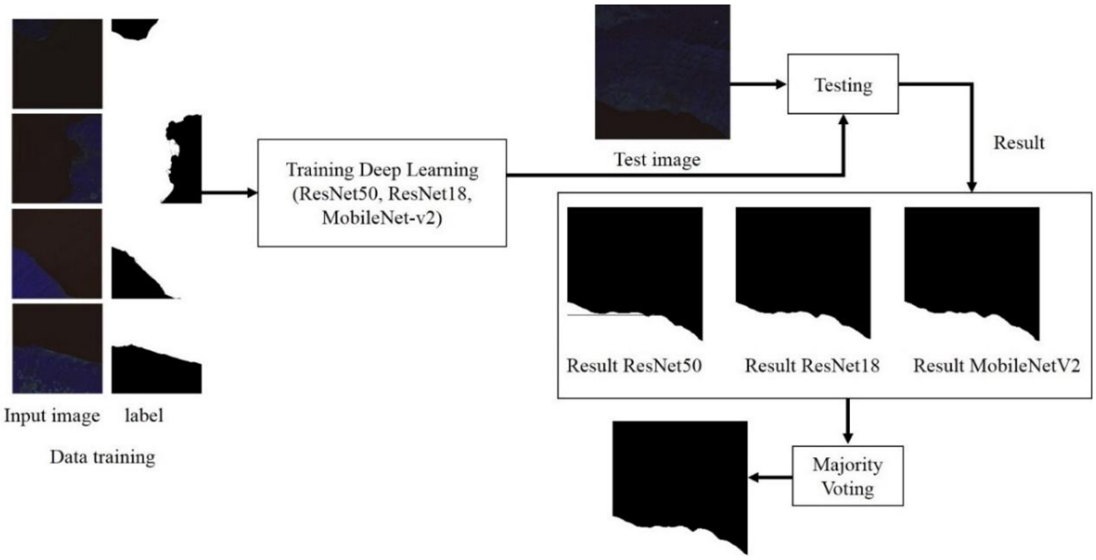

Figure 1. Segmentation process diagram

$$Jac(A,B) = \frac{|A \cap B|}{|A \cup B|} \quad (1)$$

Based on Figure 1, the model development process begins with training three deep learning architectures ResNet50, ResNet18, and MobileNet-V2 using 824 satellite images. The performance of each model was then evaluated using 20 test images to analyze their segmentation behavior. For each test image, the outputs produced by the three models were recorded, and majority voting was applied at the pixel level to generate the final segmentation result (2). Figure 2 illustrates the workflow of this majority voting process.

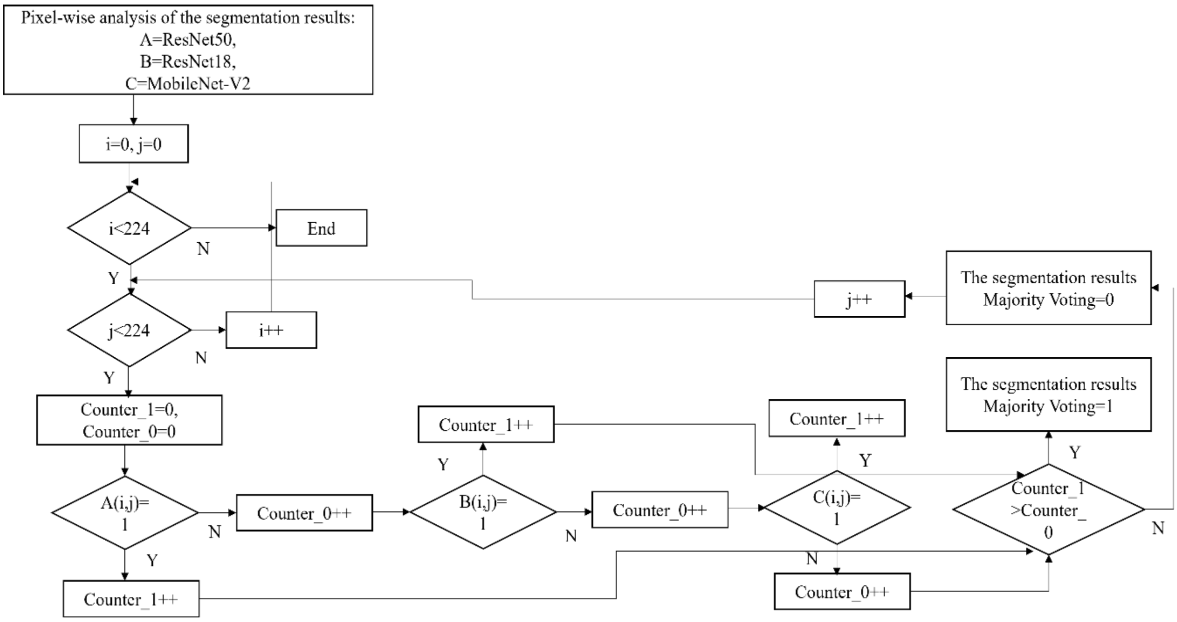

Figure 2. Majority voting segmentation flowchart

The segmentation task consists of two classes: 0 for land and 1 for seawater. In (2), H represents the final predicted label for each pixel after the voting process. Majority voting determines the pixel class based on the most frequent prediction among the three models, thereby reducing noise-related errors by leveraging the collective agreement of multiple classifiers.

$$H = \begin{Bmatrix} 1 if\ max\ c\ lass 1 to pixel i \\ 0 otherwise \end{Bmatrix} \quad (2)$$

3. RESULTS AND DISCUSSION

This study trained a total of 824 satellite images using three deep learning models: ResNet50, ResNet18, and MobileNet-V2. All models were trained using identical hyperparameters, including a learning rate (α) of 0.001, the stochastic gradient descent with momentum (SGDM) optimizer, and 40 epochs. Each model was trained three times to ensure stability and consistency of results. The average loss and accuracy obtained from these training sessions are summarized in Table 1, which shows that ResNet50 achieved the lowest loss value (0.014) and the highest accuracy (99.48%), indicating superior performance compared with ResNet18 and MobileNet-V2.

Table 1. Evaluation of the training process

No	Model	Loss	Accuracy (%)
1	ResNet50	0.014	99.48
2	ResNet18	0.016	99.38
3	MobileNet-V2	0.035	98.76

Figure 3 illustrates the training process for each deep learning model: Figure 3(a) ResNet50, Figure 3(b) ResNet18, and Figure 3(c) MobileNet-V2. These curves show changes in loss and accuracy across 40 epochs. Although the number of iterations varies depending on dataset size, the accuracy tends to stabilize after approximately 200 iterations, with minimal differences beyond that point. This pattern demonstrates that the models converge effectively within the given training configuration.

The coastline segmentation results produced by the deep learning models (ResNet50, ResNet18, and MobileNet-V2) are presented sequentially in Table 2. In this study, the Jaccard Similarity Index was used to quantify the similarity between the predicted segmentation and the ground-truth images, where values range from 0 to 1 and values closer to 1 indicate higher similarity. The segmentation results produced using the majority voting approach are shown in Table 3, while the Jaccard values for each individual model and the ensemble method are summarized in Table 4.

The majority voting method combines the outputs of all models with the aim of minimizing errors; models with higher accuracy can compensate for those with lower performance, resulting in more stable predictions. In this case, the ensemble output produced results that were not significantly different from ResNet50 for images 2, 3, 4, and 5. Although the Jaccard Similarity Index is a powerful evaluation metric, it has the limitation of being less sensitive to variations in set size, which should be considered when interpreting the results.

Based on the segmentation results of Images 1-3 in Table 2, each deep learning model exhibits specific weaknesses. The ResNet50 model produces additional boundary lines, indicating that its segmentation is not fully accurate. The ResNet18 model shows small holes and line artifacts in Images 1 and 2, suggesting instability in distinguishing land areas. Similarly, the MobileNet-V2 model generates line artifacts and missing land regions in Image 1, while Images 2 and 3 contain small holes, indicating that this model has a tendency to create gaps within land areas.

Because each individual model (ResNet50, ResNet18, and MobileNet-V2) produces different types of artifacts such as unwanted lines and holes some of these imperfections still appear in the majority voting results. However, the ensemble approach generally reduces these errors by combining the strengths of all three models. For example, although some line artifacts remain in Images 1 and 2 in Table 3, their number and prominence are reduced compared to the results produced by the individual models.

Table 3 presents five examples of Landsat 8 OLI input images along with their corresponding labels (black representing land and white representing sea). These images were segmented using the majority voting method, where the outputs from ResNet50, ResNet18, and MobileNet-V2 are combined to determine the final prediction. Overall, the majority voting method shows good average performance; however, segmentation quality decreases when the input image contains darker water regions or complex sea-land interactions. In such cases especially when the sea extends into the land area the ensemble method may still produce gaps or less accurate boundaries.

ch	Iteration	Time Elapsed (hh:mm:ss)	Mini-batch Accuracy	Mini-batch Loss	Base Learning Rate
1	1	00:01:02	52.71%	0.8066	0.0010
1	2	00:02:06	74.59%	0.5805	0.0010
1	3	00:03:11	88.18%	0.3567	0.0010
1	4	00:04:17	93.30%	0.2305	0.0010
1	5	00:05:25	95.70%	0.1547	0.0010
1	6	00:06:34	95.94%	0.1258	0.0010
2	7	00:07:43	96.09%	0.1152	0.0010
2	8	00:08:53	96.03%	0.1296	0.0010
2	9	00:10:02	96.10%	0.1262	0.0010
2	10	00:11:11	96.91%	0.1030	0.0010
2	11	00:12:21	97.53%	0.0813	0.0010
38	228	04:24:37	99.45%	0.0145	0.0010
39	229	04:25:47	99.42%	0.0155	0.0010
39	230	04:26:57	99.47%	0.0141	0.0010
39	231	04:28:07	99.46%	0.0143	0.0010
39	232	04:29:16	99.46%	0.0143	0.0010
39	233	04:30:26	99.48%	0.0142	0.0010
39	234	04:31:35	99.45%	0.0144	0.0010
40	235	04:32:45	99.42%	0.0154	0.0010
40	236	04:33:55	99.47%	0.0140	0.0010
40	237	04:35:04	99.47%	0.0141	0.0010
40	238	04:36:14	99.47%	0.0142	0.0010
40	239	04:37:24	99.48%	0.0140	0.0010
40	240	04:38:37	99.46%	0.0142	0.0010

(a)

Epoch	Iteration	Time Elapsed (hh:mm:ss)	Mini-batch Accuracy	Mini-batch Loss	Base Learning Rate
1	1	00:03:23	46.96%	0.8570	0.0010
1	2	00:06:45	68.12%	0.6313	0.0010
1	3	00:10:11	82.05%	0.4578	0.0010
1	4	00:13:26	88.10%	0.3222	0.0010
1	5	00:16:46	91.59%	0.2506	0.0010
1	6	00:20:04	93.26%	0.2031	0.0010
2	7	00:23:34	94.58%	0.1581	0.0010
2	8	00:29:03	93.78%	0.1637	0.0010
2	9	00:32:41	94.36%	0.1830	0.0010
2	10	00:36:17	94.04%	0.1771	0.0010
12	67	04:06:47	99.06%	0.0278	0.0010
12	68	04:10:22	98.93%	0.0329	0.0010
12	69	04:13:56	98.72%	0.0367	0.0010
12	70	04:17:29	98.79%	0.0363	0.0010
12	71	04:21:06	98.96%	0.0312	0.0010
12	72	04:24:41	98.87%	0.0307	0.0010
13	73	04:28:20	99.09%	0.0269	0.0010
13	74	04:31:58	98.96%	0.0313	0.0010
13	75	04:35:32	98.82%	0.0331	0.0010
13	76	04:39:08	98.84%	0.0344	0.0010
13	77	04:42:45	99.00%	0.0301	0.0010
13	78	04:46:21	98.95%	0.0291	0.0010
14	79	04:49:35	99.12%	0.0259	0.0010

(b)

Epoch	Iteration	Time Elapsed (hh:mm:ss)	Mini-batch Accuracy	Mini-batch Loss	Base Learning Rate
1	1	00:00:55	50.06%	0.9246	0.0010
1	2	00:01:56	54.12%	0.8397	0.0010
1	3	00:02:51	57.94%	0.7399	0.0010
1	4	00:03:46	66.59%	0.6235	0.0010
1	5	00:04:43	75.97%	0.5170	0.0010
1	6	00:05:43	79.07%	0.4833	0.0010
2	7	00:06:42	84.70%	0.3963	0.0010
2	8	00:07:38	86.93%	0.3552	0.0010
2	9	00:08:35	89.05%	0.3113	0.0010
2	10	00:09:31	89.78%	0.3057	0.0010
38	227	03:29:50	99.18%	0.0251	0.0010
38	228	03:30:45	99.02%	0.0292	0.0010
39	229	03:31:40	99.14%	0.0259	0.0010
39	230	03:32:35	98.91%	0.0304	0.0010
39	231	03:33:30	99.23%	0.0237	0.0010
39	232	03:34:25	98.89%	0.0321	0.0010
39	233	03:35:20	99.19%	0.0247	0.0010
39	234	03:36:15	99.04%	0.0286	0.0010
40	235	03:37:10	99.15%	0.0255	0.0010
40	236	03:38:05	98.94%	0.0297	0.0010
40	237	03:39:00	99.24%	0.0234	0.0010
40	238	03:39:55	98.91%	0.0315	0.0010
40	239	03:40:50	99.20%	0.0244	0.0010
40	240	03:41:45	99.06%	0.0281	0.0010

(c)

Figure 3. Training process (a) ResNet50, (b) ResNet18, and (c) MobileNet-V2

Based on Table 4, the Jaccard values of ResNet50 and the majority voting model are identical, indicating that the ensemble method closely mirrors the performance of the strongest individual model. Majority voting offers an advantage by reducing artifacts such as small holes or line distortions that commonly appear in single-model predictions, although this improvement requires higher computational cost because multiple models must be processed before voting is applied.

When compared with previous studies, the performance of the proposed method is generally comparable. For example, the WaterNet ensemble system in [5] achieved exceptionally high IoU and F1-scores of 99.59% and 99.79%, respectively, using a combination of U-Net variants, FC-DenseNet, and Pix2Pix. Similarly, the comparative framework in [6] reported mean IoU values above 92% when evaluating multiple state-of-the-art DCNN architectures for sea land segmentation.

Although the Jaccard values in this study are slightly lower, the findings demonstrate that a lightweight ensemble composed of ResNet50, ResNet18, and MobileNet-V2 can still produce competitive and consistent segmentation, particularly in reducing boundary noise and improving coastline stability. Thus, majority voting remains a viable alternative for scenarios that require robust segmentation with limited model complexity.

Table 2. Segmentation results

No	Input	Ground truth (label)	Result model ResNet50	Result model ResNet18	Result model MobileNet-V2
1					
2	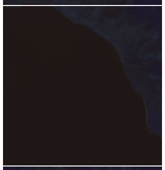				
3	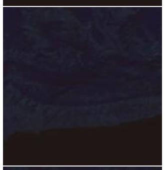				
4					
5					

Table 3. Majority voting segmentation results

No	Input	Ground truth (label)	Result majority voting
1	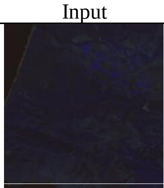		
2	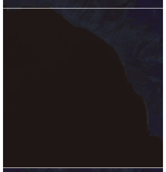		
3	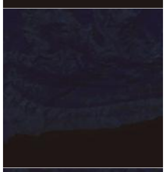		
4			
5			

This study has several limitations. First, the dataset size is relatively small and restricted to a specific geographic region, which may affect the model’s generalizability to different coastline conditions. Second, the model was trained exclusively on Landsat 8 OLI imagery, leaving its performance across other sensors (e.g., Sentinel-2, PlanetScope) unverified. Third, the majority voting ensemble increases computational cost compared with single-model approaches. Addressing these limitations will be the focus of future research.

Table 4. Model evaluation performance Jaccard

No	Model	Average
1	ResNet50	0.98
2	ResNet18	0.96
3	MobileNet-V2	0.95
4	Majority Voting (ResNet50, ResNet18, MobileNet-V2)	0.98

4. CONCLUSION

This study introduced an ensemble-based coastline segmentation approach that integrates ResNet50, ResNet18, and MobileNet-V2 using a majority voting strategy. The findings show that this ensemble provides more stable and consistent coastline boundaries than individual models, particularly by reducing boundary noise and minimizing artifacts such as small holes or line distortions. These results highlight the potential of lightweight ensembles for improving the robustness of coastline extraction in remote sensing applications.

However, this study has several limitations. The dataset size is relatively small and limited to a specific geographic region, which may restrict model generalizability. In addition, the experiments were conducted exclusively on Landsat 8 OLI imagery, leaving performance across other satellite sensors untested. The ensemble method also increases computational cost compared with single-model implementations.

Future research should therefore expand the dataset to include multiple regions, evaluate the model across different satellite sensors (e.g., Sentinel-2, PlanetScope), and investigate more efficient ensemble strategies. Applying the method to additional benchmark datasets or newly labeled coastal imagery will also help assess its adaptability to diverse shoreline conditions.

ACKNOWLEDGMENTS

Thank you to the research and service institute of Universitas Islam Lamongan, which provided the research grant.

FUNDING INFORMATION

The authors state that no funding was involved.

AUTHOR CONTRIBUTIONS STATEMENT

This journal uses the Contributor Roles Taxonomy (CRediT) to recognize individual author contributions, reduce authorship disputes, and facilitate collaboration.

Name of Author	C	M	So	Va	Fo	I	R	D	O	E	Vi	Su	P	Fu
Nur Nafiiyah	✓	✓	✓	✓					✓	✓	✓			✓
Salwa Nabilah					✓		✓	✓	✓	✓				
Nur Azizah Affandy					✓		✓		✓	✓				
Rifky Aisyatul Faroh									✓	✓				
Esa Prakasa									✓	✓		✓		

C : **C**onceptualization
M : **M**ethodology
So : **So**ftware
Va : **Va**lidation
Fo : **Fo**rmal analysis
I : **I**nvestigation
R : **R**esources
D : **D**ata Curation
O : Writing - **O**riginal Draft
E : Writing - Review & **E**diting
Vi : **Vi**sualization
Su : **Su**pervision
P : **P**roject administration
Fu : **Fu**nding acquisition

CONFLICT OF INTEREST STATEMENT

The authors state no conflict of interest.

DATA AVAILABILITY

Landsat 8 OLI (Operational Land Manager) images are publicly available on the website http://www.remotesensinglab.yildiz.edu.tr.

REFERENCES

[1] Y. Zhang and X. Hou, "Characteristics of coastline changes on Southeast Asia islands from 2000 to 2015," *Remote Sensing*, vol. 12, no. 3, p. 519, Feb. 2020, doi: 10.3390/rs12030519.

[2] C. Chen *et al.*, "The application of the tasseled cap transformation and feature knowledge for the extraction of coastline information from remote sensing images," *Advances in Space Research*, vol. 64, no. 9, pp. 1780–1791, Nov. 2019, doi: 10.1016/j.asr.2019.07.032.

[3] M. Scarpetta, M. Spadavecchia, V. I. D'Alessandro, L. De Palma, and N. Giaquinto, "A new dataset of satellite images for deep learning-based coastline measurement," in *2022 IEEE International Conference on Metrology for Extended Reality, Artificial Intelligence and Neural Engineering (MetroXRAINE)*, IEEE, Oct. 2022, pp. 635–640. doi: 10.1109/MetroXRAINE54828.2022.9967574.

[4] E. McAllister, A. Payo, A. Novellino, T. Dolphin, and E. Medina-Lopez, "Multispectral satellite imagery and machine learning for the extraction of shoreline indicators," *Coastal Engineering*, vol. 174, p. 104102, Jun. 2022, doi: 10.1016/j.coastaleng.2022.104102.

[5] F. Erdem, B. Bayram, T. Bakirman, O. C. Bayrak, and B. Akpinar, "An ensemble deep learning based shoreline segmentation approach (WaterNet) from Landsat 8 OLI images," *Advances in Space Research*, vol. 67, no. 3, pp. 964–974, Feb. 2021, doi: 10.1016/j.asr.2020.10.043.

[6] T. Yang *et al.*, "Sea-land segmentation using deep learning techniques for Landsat-8 OLI imagery," *Marine Geodesy*, vol. 43, no. 2, pp. 105–133, Mar. 2020, doi: 10.1080/01490419.2020.1713266.

[7] C. Chen, J. Fu, S. Zhang, and X. Zhao, "Coastline information extraction based on the tasseled cap transformation of Landsat-8 OLI images," *Estuarine, Coastal and Shelf Science*, vol. 217, pp. 281–291, Feb. 2019, doi: 10.1016/j.ecss.2018.10.021.

[8] Y. Liu, X. Wang, F. Ling, S. Xu, and C. Wang, "Analysis of coastline extraction from Landsat-8 OLI imagery," *Water*, vol. 9, no. 11, p. 816, Oct. 2017, doi: 10.3390/w9110816.

[9] C. Chen *et al.*, "Temporal and spatial variation of coastline using remote sensing images for Zhoushan archipelago, China," *International Journal of Applied Earth Observation and Geoinformation*, vol. 107, p. 102711, Mar. 2022, doi: 10.1016/j.jag.2022.102711.

[10] S. Hożyń and J. Zalewski, "Shoreline detection and land segmentation for autonomous surface vehicle navigation with the use of an optical system," *Sensors*, vol. 20, no. 10, p. 2799, May 2020, doi: 10.3390/s20102799.

[11] D. Cheng, G. Meng, S. Xiang, and C. Pan, "FusionNet: edge aware deep convolutional networks for semantic segmentation of remote sensing harbor images," *IEEE Journal of Selected Topics in Applied Earth Observations and Remote Sensing*, vol. 10, no. 12, pp. 5769–5783, Dec. 2017, doi: 10.1109/JSTARS.2017.2747599.

[12] A. Gao *et al.*, "A vector-based coastline shape classification approach using sequential deep learning model," *International Journal of Applied Earth Observation and Geoinformation*, vol. 129, p. 103810, May 2024, doi: 10.1016/j.jag.2024.103810.

[13] L.-C. Chen, Y. Zhu, G. Papandreou, F. Schroff, and H. Adam, "Encoder-decoder with atrous separable convolution for semantic image segmentation," in *Computer Vision – ECCV 2018*, V. Ferrari, M. Hebert, C. Sminchisescu, and Y. Weiss, Eds., Springer, Cham, 2018, pp. 833–851. doi: 10.1007/978-3-030-01234-2_49.

[14] M. Alam, J.-F. Wang, C. Guangpei, L. Yunrong, and Y. Chen, "Convolutional neural network for the semantic segmentation of remote sensing images," *Mobile Networks and Applications*, vol. 26, no. 1, pp. 200-215. 2021, doi: 10.1007/s11036-020-01703-3.

[15] K. B. Dang *et al.*, "Application of deep learning models to detect coastlines and shorelines," *Journal of Environmental Management*, vol. 320, p. 115732, Oct. 2022, doi: 10.1016/j.jenvman.2022.115732.

[16] C. Seale, T. Redfern, P. Chatfield, C. Luo, and K. Dempsey, "Coastline detection in satellite imagery: A deep learning approach on new benchmark data," *Remote Sensing of Environment*, vol. 278, p. 113044, Sep. 2022, doi: 10.1016/j.rse.2022.113044.

[17] R. Li *et al.*, "DeepUNet: a deep fully convolutional network for pixel-level sea-land segmentation," *IEEE Journal of Selected Topics in Applied Earth Observations and Remote Sensing*, vol. 11, no. 11, pp. 3954–3962, Nov. 2018, doi: 10.1109/JSTARS.2018.2833382.

[18] H. Su, S. Wei, J. Qiu, and W. Wu, "RaftNet: a new deep neural network for coastal raft aquaculture extraction from Landsat 8 OLI data," *Remote Sensing*, vol. 14, no. 18, p. 4587, Sep. 2022, doi: 10.3390/rs14184587.

[19] P. Marti-Puig, M. Serra-Serra, F. Ribas, G. Simarro, and M. Caballeria, "Automatic shoreline detection by processing planview timex images using bi-LSTM networks," *Expert Systems with Applications*, vol. 240, p. 122566, Apr. 2024, doi: 10.1016/j.eswa.2023.122566.

[20] M. Baldeon Calisto and S. K. Lai-Yuen, "AdaEn-Net: an ensemble of adaptive 2D–3D fully convolutional networks for medical image segmentation," *Neural Networks*, vol. 126, pp. 76–94, Jun. 2020, doi: 10.1016/j.neunet.2020.03.007.

[21] N. Nafi'iyah, C. Fatichah, D. Herumurti, E. R. Astuti, and R. H. Putra, "MobileNetV2 ensemble segmentation for mandibular on panoramic radiography," *International Journal of Intelligent Engineering and Systems*, vol. 16, no. 2, pp. 546–560, Feb. 2023, doi: 10.22266/ijies2023.0430.45.

[22] Z. Miao, K. Fu, H. Sun, X. Sun, and M. Yan, "Automatic water-body segmentation from high-resolution satellite images via deep networks," *IEEE Geoscience and Remote Sensing Letters*, vol. 15, no. 4, pp. 602–606, Apr. 2018, doi: 10.1109/LGRS.2018.2794545.

[23] L. Yao, D. Kanoulas, Z. Ji, and Y. Liu, "ShorelineNet: an efficient deep learning approach for shoreline semantic segmentation for unmanned surface vehicles," in *2021 IEEE/RSJ International Conference on Intelligent Robots and Systems (IROS)*, IEEE, Sep. 2021, pp. 5403–5409. doi: 10.1109/IROS51168.2021.9636614.

[24] Z. Li, R. Wang, W. Zhang, F. Hu, and L. Meng, "Multiscale features supported DeepLabV3+ optimization scheme for accurate water semantic segmentation," *IEEE Access*, vol. 7, pp. 155787–155804, 2019, doi: 10.1109/ACCESS.2019.2949635.

[25] N. Nafiiyah, C. Fatichah, D. Herumurti, E. R. Astuti, R. H. Putra, and E. Prakasa, "Mandibular segmentation on panoramic radiographs with CNN Transfer Learning," in *2022 IEEE International Conference on Communication, Networks and Satellite (COMNETSAT)*, IEEE, Nov. 2022, pp. 190–194. doi: 10.1109/COMNETSAT56033.2022.9994407.

BIOGRAPHIES OF AUTHORS

Nur Nafiiyah received her Bachelor of Informatics Engineering from Universitas Islam Lamongan, Indonesia (2005-2009) and Master of Information Technology from the Sekolah Tinggi Teknik Surabaya, Indonesia in (2011-2013). She is the Ph.D. degree in computer science with the Department of Informatics, Institut Teknologi Sepuluh Nopember 2023. She is currently interested in artificial intelligence, deep learning, and computer vision. She is currently an associate professor at the Department of Informatics at Universitas Islam Lamongan. She can be contacted at email: mynaff@unisla.ac.id.

Salwa Nabilah is currently working as an Assistant Professor in the Department of Civil Engineering, Faculty of Engineering, Universitas Islam Lamongan, Indonesia. She did her Bachelor Degree at Geomatics Engineering of Institut Teknologi Sepuluh Nopember. She continued her Master's Degree at the Department of Geomatics, Faculty of Engineering, National Cheng Kung University, Taiwan. She took the Geospatial field, which she learned about remote sensing and geospatial information systems (GIS). She also learned about measuring the field. She has almost 3 years of Teaching experience; she has published around 6 journals while working at Universitas Islam Lamongan. Her research area is Geomatics, in particular about Geospatial. She can be contacted at email: salwanabilah@unisla.ac.id.

Nur Azizah Affandy is currently working as an Assistant Professor in the Department of Civil Engineering, Faculty of Engineering, Universitas Islam Lamongan, Indonesia. She completed her undergraduate studies and earned a Bachelor of Engineering degree in 2002 in the field of Civil Engineering at the Faculty of Engineering, Universitas Islam Malang. In 2008, she pursued a Master's program in Engineering and graduated in 2011 from Institut Teknologi Sepuluh Nopember Surabaya with a concentration in Water Resources Management. In 2019, she continued her doctoral program in the same department at Institut Teknologi Sepuluh Nopember. Her research interests include water resources management, green building structure, and modeling. She can be contacted at email: nurazizah@unisla.ac.id.

Rifky Aisyatul Faroh obtained her Bachelor of Science degree from Universitas Islam Negeri Maulana Malik Ibrahim Malang, Indonesia (2012–2017), and her Master's degree in Mathematics from Universitas Brawijaya Malang, Indonesia (2017–2019). Her research interests include time series forecasting, fuzzy time series, applied statistics, and data analysis. She can be reached at rifkyaisyatulfaroh@unisla.ac.id. She can be contacted at email: rifkyaisyatulfaroh@unisla.ac.id.

Esa Prakasa has completed PhD study in Electrical and Electronics Engineering from Universiti Teknologi PETRONAS, Malaysia, in 2014. Both master and bachelor degrees have been previously finished from the University of Gadjah Mada, Yogyakarta. He has joined Research Center for Informatics, Indonesian Institute of Sciences (LIPI) since 2005. The institute is now transformed into the National Research and Innovation Agency (BRIN). His research interest is mainly in digital image processing, computer vision, and pattern recognition. He has published many research papers in international conferences and journals. He can be contacted at email: esa.prakasa@gmail.com.